ISSN (Print) 1226-1750
ISSN (Online) 2233-6656
Journal of Magnetics 30(4), 864-870 (2025) https://doi.org/10.4283/JMAG.2025.30.4.864

Clinical Significance Myocardial Extracellular Volume Quantification by Cardiac Computed Tomography in Cardiomyopathy: Comparison with Magnetic Resonance Imaging

Sung-Jin Cha[1,2] and Pil-Hyun Jeon[3]*

[1]*Department of Radiation Convergence Engineering, Yonsei University, Wonju 26493, Gangwon-do, Republic of Korea*
[2]*Department of Radiology, Yonsei University, Wonju Severance Christian Hospital, Wonju 26424, Gangwon-do, Republic of Korea*
[3]*Department of Radiological Science, Dawon University, Jecheon 27135, Chungcheong Buk-do, Republic of Korea*

(Received 7 November 2025, Received in final form 23 December 2025, Accepted 24 December 2025)

Myocardial extracellular volume (ECV) is an important parameter for assessing the pathophysiology of cardiomyopathy, and cardiac magnetic resonance imaging (CMR) is established as the standard technique for its measurement. However, CMR has several clinical limitations, creating a need for alternative imaging modalities. Cardiac computed tomography (CT) has emerged as a potential alternative. The primary aim of this study was to directly compare the accuracy and agreement of myocardial ECV measured by cardiac CT (CT-ECV) and by CMR (MRI-ECV) in the same patient cohort. In this retrospective study, 44 patients were included, all of whom underwent both cardiac CT and CMR. Statistical analyses, including paired t-tests and Pearson correlation, were performed to compare ECV values obtained by the two techniques. In the overall cohort, the mean MRI-ECV was 26.27%, and the mean CT-ECV was 26.57%. The mean difference between the two modalities was not statistically significant (p = 0.279). A strong positive correlation was observed between CT-ECV and MRI-ECV values (r = 0.776). CT-ECV demonstrated a high degree of correlation and agreement with the CMR reference standard, suggesting that CT-ECV may serve as a reliable, accurate, and clinically practical alternative for myocardial tissue characterization in patients with cardiomyopathy.

Keywords : cardiac computed tomography, cardiac magnetic resonance imaging, T1 mapping, myocardial extracellular volume, cardiopathy

1. Introduction

Cardiomyopathy encompasses a diverse group of heart muscle disorders often leading to heart failure or sudden cardiac death. Despite varied causes, a common hallmark is myocardial fibrosis – the excessive accumulation of extracellular matrix (primarily collagen) within the myocardium [1]. This fibrotic remodeling increases myocardial stiffness, disrupts electrical conduction, and ultimately impairs cardiac function. Myocardial extracellular volume (ECV) fraction is a quantitative marker of this process, representing the proportion of myocardial tissue volume occupied by extracellular space [2]. In healthy hearts this space is minimal, but in cardiomyopathies it expands due to diffuse interstitial fibrosis (or other extracellular deposits such as amyloid or edema). An elevated ECV indicates diffuse myocardial disease and often appears before changes in ejection fraction or focal scar become evident. Moreover, high ECV has proven prognostic significance, correlating with worse outcomes, independent of conventional measures like left ventricular ejection fraction (LVEF) or late gadolinium enhancement (LGE). These attributes make ECV an attractive early biomarker and therapeutic monitoring tool in cardiology [1, 3].

Currently, cardiac magnetic resonance (CMR) with T1 mapping is the noninvasive gold standard for measuring myocardial ECV [3] . By comparing pre-contrast and post-contrast T1 relaxation times in myocardium and blood (with adjustment for hematocrit), CMR can accurately calculate the ECV fraction. This method leverages gadolinium-based contrast agents that distribute exclusively into the extracellular space, and it has been validated against histological collagen quantification.

*Corresponding author: Tel: +82-43-649-3301
e-mail: iromeo138@naver.com

However, despite its accuracy, CMR has practical limitations. Scans typically exceed 30 minutes and require breath-holding, the equipment is expensive and less available outside specialized centers, and certain patients (e.g. those with incompatible implants or severe claustrophobia) cannot undergo MRI [4]. These factors constrain the widespread use of CMR-based tissue characterization, creating a need for a more accessible alternative to quantify myocardial fibrosis in routine clinical practice [5, 6, 7].

Cardiac computed tomography (CT) has emerged as a promising alternative for ECV quantification that could overcome these barriers. CT uses iodine-based contrast agents which, like gadolinium, remain in the extracellular space. By measuring the change in myocardial Hounsfield units (HU) between an unenhanced scan and a delayed post-contrast scan (and correcting for blood pool enhancement and hematocrit), CT can derive the myocardial ECV fraction in a manner analogous to CMR [8]. The approach is highly appealing from a clinical feasibility standpoint. CT scans are rapid (often just a few minutes), widely available in most hospitals, and relatively cost-effective. Importantly, CT imposes no restrictions on patients with pacemakers, defibrillators, or other metallic implants. This means critically ill patients or those ineligible for MRI can still undergo CT-based ECV assessment [9, 10]. Additionally, ECV mapping can be conveniently added to routine CT examinations—such as a coronary CT angiography or pre-procedural planning CT for valve interventions—without significant extra contrast or scan time. In a single session, CT can thus provide both detailed anatomic information and tissue characterization, streamlining the diagnostic workflow [11]. These advantages suggest that CT-based ECV measurement could greatly improve access to myocardial tissue characterization, if its accuracy and reliability are proven comparable to the MRI reference standard [12].

Early evidence supporting CT-ECV is encouraging. Several studies, including systematic reviews and meta-analyses, have reported an excellent agreement between CT-derived and MRI-derived ECV values [13-15]. Pooled analyses across diverse patient populations show a very strong correlation (around $r \approx 0.90$) between the two modalities, with mean differences often less than 1 percentage point. This strong concordance provides a theoretical basis that CT can serve as a valid surrogate for MRI in quantifying diffuse myocardial fibrosis. However, these meta-analytic findings represent aggregate data [14]. Direct head-to-head comparisons in specific patient cohorts remain essential to validate CT's performance under uniform conditions and to build clinical confidence in its use. In particular, for patients with cardiomyopathy – who stand to benefit from early fibrosis detection – it is crucial to confirm that CT can reliably quantify ECV in alignment with the MRI gold standard [16, 17].

The present study was designed to rigorously compare CT-based ECV quantification with the established CMR-based ECV in a cohort of patients with cardiomyopathy, examining both reliability and agreement between the two methods. The present study hypothesized that myocardial ECV measured by CT would show no significant difference compared with MRI-derived ECV and would demonstrate a strong correlation.

2. Materials and Methods

2.1. Study Population and design

This single-center retrospective comparative study was approved by our Institutional Review Board (IRB No. CR320058). The study population consisted of patients who presented with cardiomyopathy and underwent both cardiac CT and cardiac MRI as part of their clinical evaluation between June 2020 and June 2023. Patients with severe imaging artifacts, those who did not complete both the CT and MRI protocols, and pediatric patients were excluded from the analysis. A total of 44 patients were ultimately included in the final analysis (Fig. 1).

2.2. Cardiac CT image acquisition and ECV quantification

All CT examinations were performed using a dual-

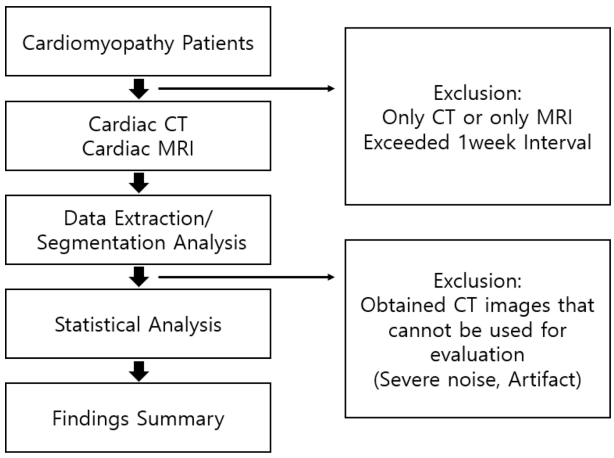

Fig. 1. Schematic workflow of the study design and analysis. This figure illustrates the patient selection process and the overall study workflow, including cardiac CT and cardiac MRI acquisition, myocardial extracellular volume (ECV) quantification using both modalities, and statistical comparison of CT-derived and MRI-derived ECV values at global and segmental levels.

Table 1. Cardiac CT angiography acquisition parameters used for CT-based myocardial ECV quantification. The standardized scan protocol was designed to ensure consistent attenuation measurements between pre-contrast and delayed post-contrast images, enabling accurate calculation of myocardial extracellular volume.

Protocol	CCTA
mAs	CARE Dose4D
kV	Qualify Ref. 100kV
Rotation Time	0.25 sec
Kernel	Bv40
Collimation	96 × 0.6 mm
Delay time	7 sec
Thickness/Increment	0.6 / 0.4 mm

source 2 × 192-slice CT scanner (Somatom Force, Siemens Healthineers). The scan parameters used in this study are shown in Table 1. The acquisition protocol was standardized to enable accurate calculation of extracellular volume (ECV) and consisted of the following multistep procedure:

A low-dose, non-contrast pre-contrast scan was first acquired to measure the baseline attenuation (HU values) of the myocardium and blood pool, followed by standard coronary CT angiography (CCTA) after intravenous administration of 60 mL of iodinated contrast material (iopromide, Ultravist 370) at a flow rate of 4.5 mL/s. To allow equilibrium of contrast medium between the intravascular and interstitial spaces, delayed-phase images were then obtained 5 minutes after contrast injection using the same parameters as the pre-contrast scan; this delay time is critical for accurate ECV calculation.

Image post-processing and analysis were performed on a dedicated commercial workstation (Syngo.via, Siemens Healthineers). Short-axis (SA) images were reconstructed from both the pre-contrast and delayed-phase datasets, and circular regions of interest (ROIs) with an area of 10 mm² were placed in the myocardium and left ventricular blood pool at corresponding locations. Myocardial ROIs were positioned according to the 17-segment model of the American Heart Association (AHA) in segments 7–12 at the mid-ventricular level (anterior, anteroseptal, inferoseptal, inferior, inferolateral, and anterolateral walls). The ROIs were independently placed by two radiologic technologists, and HU values from each observer were averaged and used to manually calculate ECV (Fig. 2).

CT-ECV was calculated using the following standard formula (1).

$$\text{ECV}(\%) = (1\text{-Hematocrit}) \times \frac{\Delta HU_{myocardium}}{\Delta HU_{blood\ pool}} \quad (1)$$

Here, the change in Hounsfield units is defined as Δ; the post-contrast HU value minus pre-contrast HU value [8].

2.3. Cardiac MRI image acquisition and ECV quantification

All patients underwent cardiac MRI in addition to cardiac CT. ECV measurement by MRI is currently regarded as the clinical standard and was used as the reference standard in this study. CMR was performed on a 3.0-T MRI scanner (Magnetom Vida; Siemens Healthineers, Erlangen, Germany) using a 32-channel cardiac phased-array coil. Native and post-contrast T1 mapping were acquired in four short-axis slices from base to apex with a voxel size of 1.5 × 1.5 × 8.0 mm³, using a vendor-provided, inversion-recovery–based, ECG-triggered balanced steady-state free precession (bSSFP/TrueFISP) readout. Native T1 maps were obtained with TR/TE of

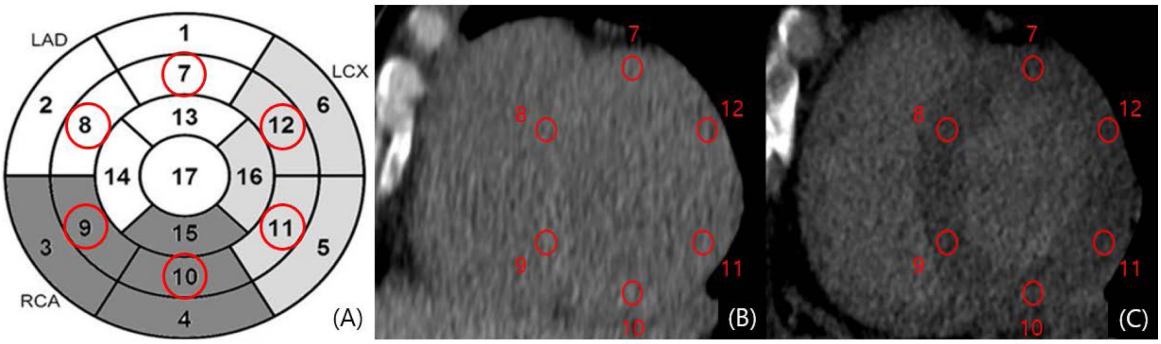

Fig. 2. (Color online) (A) AHA 17 segment model (segments 7–12: anterior, anteroseptal, inferoseptal, inferior, inferolateral, and anterolateral walls) highlighted in red circles, (B) Pre-contrast short-axis CT image at the mid-ventricular level showing circular 10-mm² regions of interest (ROIs) placed in each of the six myocardial segments, (C) Corresponding delayed-phase short-axis CT image with ROIs placed at identical locations for paired measurement of pre- and post-contrast attenuation used for ECV calculation.

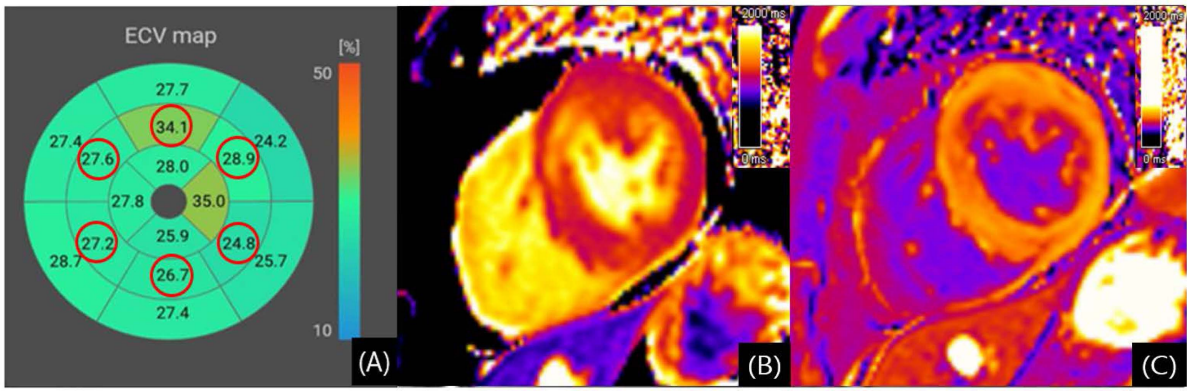

Fig. 3. (Color online) (A) Polar ECV map generated from T1 mapping, with the six mid-ventricular segments (AHA segments 7–12) outlined in red and segmental ECV values displayed as percentages. (B) Native (pre-contrast) short-axis T1 map at the mid-ventricular level. (C) Corresponding post-contrast short-axis T1 map acquired in the equilibrium phase after gadolinium administration. B and C are images from a 56-year-old male patient with hypertrophic cardiomyopathy.

327.3/1.03 ms and a flip angle of 35°, and post-contrast T1 maps with TR/TE of 368.1/1.03 ms and the same flip angle. For both T1-mapping acquisitions, GRAPPA parallel imaging with an acceleration factor of 2 and 7/8 phase partial Fourier were applied. Post-contrast T1 maps were acquired 10 minutes after intravenous administration of 0.1 mmol/kg gadoterate meglumine (Dotarem; Guerbet, Aulnay, France). T1 maps and T1 mapping–derived extracellular volume fraction maps were generated on a dedicated post-processing workstation (Myomics v.2.0.2.12; Phantomics), which was used to generate ECV maps and quantify segmental ECV values (Fig. 3). The MRI-derived ECV formula is similar to the CT-based formula, except that it uses the change in T1 relaxation rate (ΔR1, where R1 = 1/T1) instead of HU values [2].

2.4. Statistical Analysis

The statistical analysis was performed using the Statistical Package for the Social Sciences (SPSS, version 29.0; IBM, Armonk, NY, USA). To compare the mean ECV values measured by CT and MRI, a paired t-test was performed. Pearson correlation analysis was conducted to evaluate the correlation between the two measurement techniques. The strength of the correlation was assessed based on the absolute value of the Pearson correlation coefficient (r), and was interpreted as follows: 0.00–0.19, very weak; 0.20–0.39, weak; 0.40–0.59, moderate; 0.60–0.79, strong; and 0.80–1.0, very strong. A p-value < 0.05 was considered statistically significant.

3. Results and Discussion

The final study cohort included 44 patients who successfully underwent both cardiac CT and MRI. The demographic and baseline characteristics of the patients are summarized in Table 2. The mean age was 49.11 years, 28 patients were male, and the mean hematocrit was 38.95%.

Table 2. Baseline demographic and clinical characteristics of the study population.

Characteristic	
Number of patients	44
Age, y	49.11 ± 17.03
Sex(men)	28
Height(m)	1.69 ± 0.08
Weight(kg)	72.05 ± 14.37
BMI	25.11 ± 3.7
Hematocrit(%)	38.95 ± 4.56

Values are presented as mean ± standard deviation. A total of 44 patients who underwent both cardiac CT and cardiac MRI were included in the final analysis.

For the primary endpoint of the study, the overall myocardial ECV values were compared between modalities. The mean ECV quantified by MRI was 26.27%, whereas the mean ECV quantified by CT was 26.57%. The mean difference between the two measurements was not statistically significant ($p = 0.279$). These results are visually presented as a boxplot in Fig. 4. To confirm that this overall agreement was not simply the result of regional differences averaging out, the analysis was extended to a regional level by comparing ECV values within the six mid-ventricular myocardial segments (AHA segments 7–12). The mean ECV values for each segment are presented in Table 3. For example, in segment 7 (anterior wall), the mean MRI-derived ECV was 25.33% and the mean CT-derived ECV was 24.87%, while in

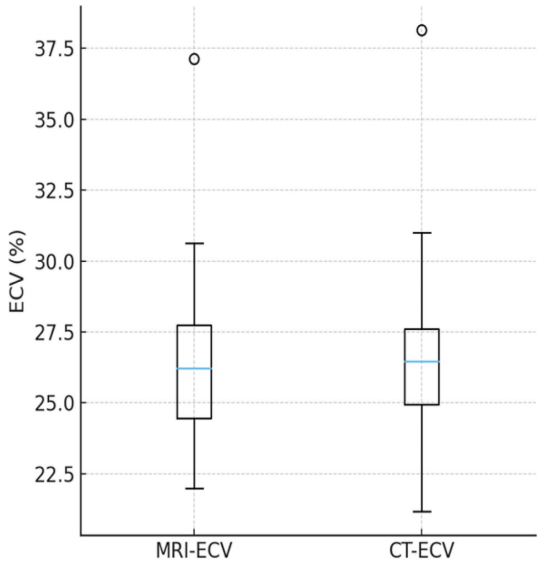

Fig. 4. (Color online) Box-and-whisker plots of global myocardial extracellular volume (ECV) measured by MRI and CT. The distributions of MRI-derived and CT-derived ECV are similar, with comparable central tendency and spread; CT shows slightly higher values overall. Boxes represent the interquartile range with the median line, whiskers indicate 1.5× the interquartile range, and circles denote outliers. The difference in global mean ECV between MRI and CT was not statistically significant (p = 0.279).

segment 8 (anteroseptal wall), the corresponding values were 26.76% and 27.67%, respectively. Paired t-test analysis showed no statistically significant differences between CT- and MRI-derived ECV values in any of the individual segments (all p-values > 0.05). Although segments 8 and 9 showed a trend toward slightly higher CT-derived ECV values compared with MRI, these differences did not reach statistical significance.

This study evaluated the feasibility of myocardial extracellular volume (ECV) quantification using cardiac CT by directly comparing it with CMR as the reference standard. Three principal findings emerged: (1) there was no statistically significant difference between the global mean ECV values measured by CT and MRI; (2) this agreement was maintained at the regional level across the six mid-ventricular myocardial segments; and (3) Pearson correlation analysis demonstrated a strong correlation between CT- and MRI-derived global ECV values (r = 0.776). Taken together, these results support cardiac CT as an accurate and reliable modality for quantitative assessment of myocardial ECV (Fig. 5).

These findings are consistent with previous systematic reviews and meta-analyses. Han et al. reported a pooled correlation coefficient of 0.90 between CT-derived and MRI-derived ECV and a small pooled mean difference of 0.96%, indicating a slight tendency for CT to overestimate ECV relative to MRI [14]. The strong correlation and the mildly higher, though not statistically significant, CT-derived ECV values observed in the present study are in line with these results, reinforcing the validity and potential generalizability of CT-based ECV quantification. Although a dual-source CT system was used in this study, prior data suggest that both single-energy and dual-energy CT can provide clinically acceptable ECV estimates, without a meaningful difference in mean ECV values between techniques [15, 16, 18].

From a clinical perspective, CT-ECV offers several important advantages. It can expand access to myocardial tissue characterization in patients with contraindications to MRI or limited access to advanced CMR facilities [10, 13]. CT also enables a “one-stop” cardiac examination in which coronary anatomy, ventricular function, and myocardial tissue characteristics can be assessed in a single visit, thereby improving workflow efficiency and reducing patient burden [19]. Furthermore, ECV can be measured

Table 3. Segment-wise comparison of myocardial extracellular volume (ECV) measured by cardiac MRI and cardiac CT at the mid-ventricular level.

Segment	ECV_{MR}	ECV_{CT}	p-value	r(Pearson)
Anterior(S7)	25.33 ± 2.58	24.87 ± 3.57	0.368	0.444
Anteroseptal(S8)	26.76 ± 3.16	27.67 ± 3.28	0.057	0.546
Inferoseptal(S9)	26.96 ± 2.80	27.86 ± 4.13	0.094	0.557
Inferior(S10)	26.64 ± 2.70	26.97 ± 4.05	0.527	0.541
Inferolateral(S11)	25.84 ± 2.86	26.58 ± 4.82	0.219	0.578
Anterolateral(S12)	26.08 ± 2.57	25.45 ± 3.64	0.337	0.444
Average(S7~12)	26.27 ± 2.63	26.57 ± 2.74	0.279	0.776

Mean ECV values for AHA segments 7–12 are presented for both modalities. No statistically significant differences were observed between CT-derived and MRI-derived ECV values in any segment. Pearson correlation coefficients indicate moderate to strong correlations across segments, with strong agreement for averaged ECV values.

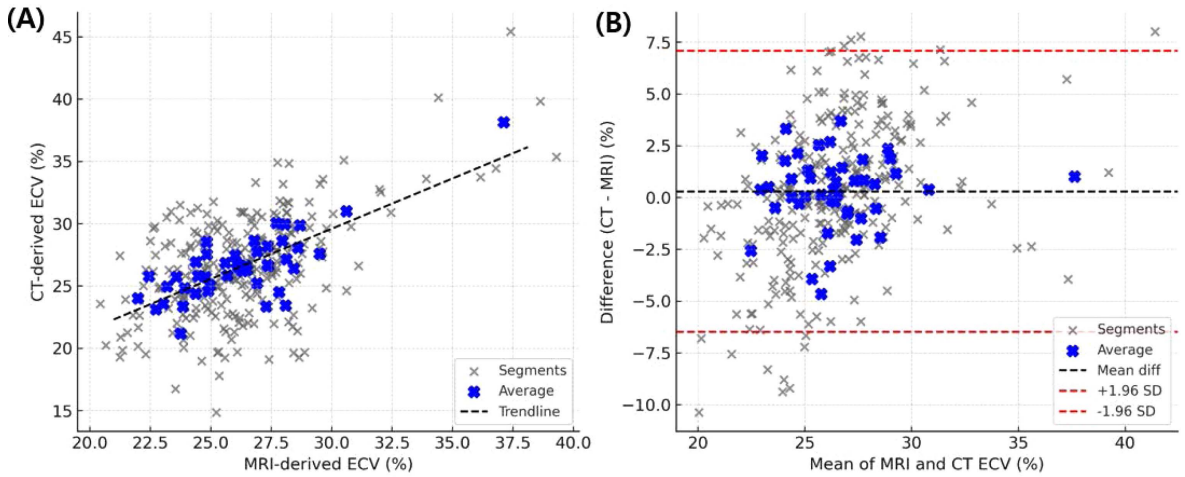

Fig. 5. (Color online) Comparison between CT-derived and MRI-derived ECV values. (A) Scatter plot showing the Pearson correlation between CT-derived and MRI-derived extracellular volume fraction (ECV). Blue crosses represent average ECV values calculated from six mid-ventricular segments (S7–S12), while gray crosses indicate individual segment-level data. The dotted line indicates the linear regression trendline. (B) Bland-Altman plot demonstrates the agreement between CT- and MRI-derived average ECV values. The mean difference (black dashed line) and 95% limits of agreement (±1.96 SD, red dashed lines) are displayed. Blue crosses indicate the average values for each patient, and gray crosses represent individual segment values.

opportunistically during CT examinations performed for other indications (e.g., chest pain evaluation or TAVR planning), allowing incidental detection of diffuse myocardial fibrosis that might otherwise remain unrecognized [20, 21].

Beyond its diagnostic role, CT-ECV has emerging prognostic significance. Previous studies have demonstrated that elevated CT-ECV is associated with an increased risk of major adverse cardiac events in hypertrophic cardiomyopathy and with unfavorable post-procedural outcomes in severe aortic stenosis [20]. These data suggest that CT-derived ECV, similar to MRI-derived ECV, may be useful for risk stratification and for guiding therapeutic decision-making.

Several limitations of this study should be acknowledged. First, this was a retrospective, single-center analysis with a relatively small sample size (n = 44), which may limit statistical power and generalizability. Second, the findings may not be directly applicable to institutions using different scanners or imaging protocols, and the study population was restricted to a specific cardiomyopathy cohort, warranting further validation in other etiologies of myocardial disease. Third, unlike previous studies that have used automated or segment-based analysis to derive CT-ECV, our measurements were obtained from manually placed circular ROIs, which are susceptible to sampling bias and observer dependence and may not fully represent the entire myocardial segment. Finally, subtle spatial mismatches in ROI placement between pre- and post-contrast images may have introduced additional measurement variability. Future large-scale, prospective, multicenter studies with standardized CT protocols, as well as investigations incorporating newer technologies such as photon-counting CT, will be essential to refine CT-ECV thresholds and to more clearly define its prognostic and clinical utility [22, 23].

4. Conclusion

This study provides direct evidence that myocardial extracellular volume quantification using cardiac CT shows excellent agreement with CMR, the current reference standard, with no significant global or regional differences in mean ECV values and a strong correlation between the two modalities.

Given its shorter examination time, lower cost, wider availability, and fewer contraindications, CT-derived ECV may be particularly useful in centers without access to advanced cardiac MRI or in patients with contraindications to MRI, offering a practical alternative for myocardial tissue. Integration of CT-ECV into routine practice may improve diagnosis, risk stratification, and management across a broad spectrum of cardiomyopathies. Further large-scale studies are warranted to establish its definitive role in clinical decision-making and long-term prognostic assessment.

References

[1] T. A. Treibel, Y. Fridman, P. Bering, A. Sayeed, M. Maanja, F. Frojdh, L. Niklasson, E. Olausson, T. C. Wong, P. Kellman, C. A. Miller, J. C. Moon, M. Ugander, and E. B. Schelbert, JACC Cardiovasc Imaging **13**, 44 (2020).

[2] H. Zhang, W. Yang, D. Zhou, Y. Wang, L. Zhu, M. Jiang, Q. Zhang, A. Sirajuddin, A. E. Arai, S. Zhoo, and M. Lu, JACC Cardiovasc Imaging **18**, 1203 (2025).

[3] S. K. White, D. M. Sado, M. Fontana, S. M. Banypersad, V. Maestrini, A. S. Flett, S. K. Piechnik, M. D. Robson, D. J. Hausenloy, A. M. Sheikh, P. N. Hawkins, and J. C. Moon, JACC Cardiovasc Imaging **6**, 955 (2013).

[4] D. M. Sado, A. S. Flett, S. M. Banypersad, S. K. White, V. Maestrini, G. Quarta, R. H. Lachmann, E. Murphy, A. Mehta, D. A. Hughes, W. J. McKenna, A. M. Taylor, D. J. Hausenloy, P. N. Hawkins, P. M. Elliott, and J. C. Moon, Heart **98**, 1436 (2012).

[5] C. A. Miller, J. H. Naish, P. Bishop, G. Coutts, D. Clark, S. Zhao, S. G. Ray, N. Yonan, S. G. Williams, A. S. Flett, J. C. Moom, A. Greiser, G. J. Parker, and M. Schmitt, Circ Cardiovasc Imaging **6**, 373 (2013).

[6] A. A. Kammerlander, B. A. Marzluf, C. Z. Tufaro, S. Aschauer, F. Duca, A. Bachmann, K. Knechtelsdorfer, M. Wiesinger, S. Pfaffenberger, A. Greiser, I. M. Lang, D. Bonderman, and J. Mascherbauer, JACC Cardiovasc Imaging **9**, 14 (2016).

[7] C. W. Yancy, M. Jessup, B. Bozkurt, J. Butler, D. E. Casey, M. H. Drazner, G. C. Fonarow, S. A. Geraci, T. Horwich, J. L. Januzzi, M. R. Johnson, E. K. Kasper, W. C. Levy, F. A. Masoudi, P. E. McBride, J. V. McMurray, J. E. Mitchell, P. N. Peterson, B. Riegel, F. Sam, L. W. Stevenson, W. H. Wilson, E. J. Tsai, and B. L. Wilkoff, J. Am. Coll. Cardiol. **62**, e147 (2013).

[8] M. S. Nacif, N. Kawel, J. J. Lee, X. Chen, J. Yao, A. Zavodni, C. T. Sibley, J. C. Lima, S. Liu, and D. A. Bluemke, Radiology **264**, 876 (2012).

[9] H. S. Thomsen, Eur. Radiol. **16**, 2619 (2006).

[10] A. Tang, R. Tam, A. Cadrin, W. Guest, J. Chong, J. Barfett, L. Chepelev, R. Cairns, J. R. Mitchell, M. D. Cicero, M. G. Poudrette, J. L. Jaremko, C. Reinhoid, B. Gallix, B. Gray, and R. Geis, Can. Assoc. Radiol. J **69**, 26 (2018).

[11] S. Paleri, C. Rayner, T. Abrahams, S. Vasanthakumar, V. Goel, R. Muthalaly, A. Lin, and N. Nerlekar, Curr Cardiovasc Imaging Rep. **18**, 8 (2025).

[12] A. Hamdy, K. Kitagawa, Y. Goto, A. Yamada, S. Nakamura, M. Takafuji, N. Nagasawa, and H. Sakuma, J. Comput. Assist. Tomogr. **35**, 917 (2019).

[13] P. Kellman, J. R. Wilson, H. Xue, M. Ugander, and A. E. Arai, J. Cardiovasc. Magn. Reson. **14**, 63 (2012).

[14] D. Han, A. Lin, K. Kuronuma, H. Gransar, D. Dey, J. D. Friedman, D. S. Berman, and B. K. Tamarappoo, JACC Cardiovasc Imaging **16**, 1306 (2023).

[15] H. Zhang, Z. H. Guo, G. Liu, C. Wu, Y. Ma, S. Li, Y. Zheng, and J. Zhang, Eur. Radiol. **33**, 8464 (2023).

[16] S. Kato, Y. Misumi, N. Horita, K. Yamamoto, and D. Utsunomiya, JACC Cardiovasc Imaging **17**, 516 (2024).

[17] J. S. Wolter, J. M. Treiber, S. Fischer, U. Fischer, S. D. Kriechbaum, A. Rieth, M. Weferling, B. V. Jeinsen, A. Hain, C. W. Hamm, T. Keller, and A. Rolf, Diagnostics **13**, 2240 (2023).

[18] A. Faggiano, E. Gherbesi, S. Carugo, M. Brusamolino, D. A. Cozac, M. T. Savo, F. Cannata, M. Guglielmo, L. L. Mura, F. Fazzari, N. Carrabba, E. Conte, S. Mushtaq, A. Baggiano, A. I. Guaricci, R. Pedrinelli, C. Indolfi, G. Sinagra, P. P. Filardi, V. Pergola, and G. Pontone, Eur. Heart J. Cardiovasc. Imaging **26**, 518 (2025).

[19] T. A. Treibel, R. Kozor, R. Schofield, G. Benedetti, M. Fontana, A. N. Bhuva, A. Sheikh, B. Lopez, A. Gonzalez, C. Manisty, G. Lloyd, P. Kellman, J. Diez, and J. C. Moon, J. Am. Coll. Cardiol. **71**, 860 (2018).

[20] M. H. Drazner, B. Bozkurt, L. T. Cooper, N. R. Aggarwal, C. Basso, N. M. Bhave, A. L. Caforio, V. M. Ferreira, B. Heidecker, A. R. Kontorovich, P. Martin, G. A. Roth, and J. E. Van Eyk, J. Am. Coll. Cardiol. **85**, 391 (2025).

[21] T. Kotecha, L. Chacko, O. Chehab, N. O'Reilly, A. M. Naharro, J. Lazari, K. D. Knott, J. Brown, D. Knight, V. Muthurangu, P. Hawkins, S. Plein, J. C. Moon, H. Xue, P. Kellman, R. Rakhit, N. Patel, and M. Fontana, JACC Cardiovasc Imaging **13**, 2544 (2024).

[22] M. T. Hagar, W. G. Moore, M. Vecsey-Nagy, J. Osoria-Velasquez, J. Griggers, F. Bamberg, A. Vargo-Szemes, and T. Emrich, Eur. Radiol. **191**, e112321 (2025).

[23] G. J. Aquino, J. O'Doherty, U. J. Schoepf, B. Ellison, J. Byrne, N. Fink, E. Zsarnoczay, E. V. Wolf, T. Allmendinger, B. Schmidt, T. Flohr, D. Baruah, P. Suranyi, A. Varga-Szemes, and T. Emrich, Radiology **307**, e222030 (2023).